Preparation and characterization of an inorganic magnesium chloride/nitrate/graphite composite for low temperature energy storage

Yana Galazutdinova[1], Mariela Vega[2], Mario Grágeda[1], Luisa F. Cabeza[3], Svetlana Ushak[1*]

[1] Department of Chemical Engineering and Mineral Processing and Center for Advanced Study of Lithium and Industrial Minerals (CELiMIN), Universidad de Antofagasta, Campus Coloso, Av. Universidad de Antofagasta 02800, Antofagasta, Chile.

[2] Universidad Mayor de San Simón, Facultad de Ciencias y Tecnología, Cochabamba, Bolivia.

[3] GREA Innovació Concurrent, INSPIRES Research Centre, Universitat de Lleida, Pere de Cabrera s/n, 25001, Lleida, Spain.

*corresponding author: svetlana.ushak@uantof.cl, tel. 56-552637312, fax 56-552637801

Abstract

In this study, an inorganic mixture of 40 wt.% $MgCl_2 \cdot 6H_2O$ and 60 wt.% $Mg(NO_3)_2 \cdot 6H_2O$ was impregnated into two types of the expanded graphite (EG): EG flakes and EG matrix. Different methods of preparation usually used in the organic composite preparation, such as direct blending, vacuum impregnation, ultrasonic impregnation and immersion were applied in this work. Considering the samples with EG matrix, it can be concluded that the optimal result of the encapsulation and ΔH ratio can be reached with the experimental time of 1, 3 and 4 hours using the vacuum, ultrasound and immersion methods, respectively. Moreover, the percentage of encapsulation increases with the experimental time and with the EG percentage for the EG matrix and for the EG flakes, respectively. Concerning the supercooling phenomena, the results show that the presence of EG reduces the difference between fusion and crystallization temperature for up to 65%, acting as a nucleating agent. The resulting composite samples (CPCM) were proved to have good latent heat and a significant reduction of the supercooling effect, which eliminates the need to use nucleating agents, that are essential for pure PCM of 40 wt.% $MgCl_2 \cdot 6H_2O$ and 60 wt.% $Mg(NO_3)_2 \cdot 6H_2O$. Moreover, using EG suppresses significantly the melting time which indicates the heat transfer enhance of the mixture. This circumstance could allow to empower the utilization of the mentioned mixture in different fields of thermal energy storage at low temperature.

Keywords: inorganic phase change material, expanded graphite, heat transfer enhancement, composite material.

1. Introduction

Under today's increase of energy demand, using phase change materials is one of the most promising methods for thermal energy storage. The energy is stored as a combination of sensible and latent heat. During the process of phase change, thermal energy is absorbed or released at a

constant temperature which allows to control temperature during the thermal energy storage (TES) process.

Inorganic salt hydrates are particularly convenient as materials for low temperature TES. However, one of the main problems of their use is supercooling due to weak nucleating properties. At the melting temperature, nucleation rate in most of the cases is very low. That is why, to reach a reasonable nucleation rate, the solution has to be supercooled and thus the energy is being discharged at much lower temperature. Thereby, a liquid crystallizes much below its melting point. G. Lane [1] indicated that this effect is not acceptable because this reduces the utility of the material, and if too severe, can completely prevent heat recovery. Many factors determine whether an additive will promote nucleation: crystal structure, solubility, and hydrate stability are some of them. Such additives are called nucleating agents. The criteria to choose the nucleating agent was described and reported by different authors [1,2]. Based on these investigations, the best nucleating agents will have similar crystallographic parameters to the material under study, stable structure and stable state under the working conditions. Furthermore, for heterogeneous nucleation the nucleating agent must have lower solubility in water, higher melting point and must bind water in its structure.

Another important problem of inorganic PCM is that of low heat charging and discharging rates due to their low thermal conductivity. So far, the methods carried out to enhance heat transfer in energy storage systems include adding finned configurations, dispersing high conductivity particles (metal, ceramic, graphite, graphene), impregnating a porous matrix (metallic or carbon), and encapsulating the material [3-5]. Among them, expanded graphite (EG) with porous structure was proved to be an excellent heat fortifier to improve heat transfer of materials. EG can be easily obtained from the graphite flakes, reaching a high external heat transfer coefficient, low bulk density, resistance to corrosion and chemical stability [6-8]. Currently, there are many research works dealing with the preparation of composite materials using EG and PCM. However, almost all of them employ organic PCM [9-18] and there are only two studies that prepare composite with inorganic PCM for medium [19] and high [20] temperature applications.

According to the provided literature, there is still a lack of understanding on developing of the EG/inorganic PCM composite. To help reduce this knowledge gap, this work reports the results of the preparation of composite materials, using an inorganic mixture of 40 wt.% $MgCl_2 \cdot 6H_2O$ and 60 wt.% $Mg(NO_3)_2 \cdot 6H_2O$.

Binary magnesium nitrate/magnesium chloride mixtures with different compositions are well-studied and characterized in literature as phase change materials [21-26]. The literature review indicates that it is possible to obtain a number of mixtures $MgCl_2 \cdot 6H_2O/Mg(NO_3)_2 \cdot 6H_2O$ with various fusion temperatures and heat of fusion, some of which are reported as eutectic, and have potential to be used as PCM. Available literature data related to the mixture of $MgCl_2 \cdot 6H_2O$ and $Mg(NO_3)_2 \cdot 6H_2O$ is summarized in Table 1.

Table 1. Literature data for $MgCl_2 \cdot 6H_2O/Mg(NO_3)_2 \cdot 6H_2O$ mixtures studied as PCM.

wt.% of $MgCl_2 \cdot 6H_2O$	T_f, °C	ΔH_f, kJ·kg^{-1}	Reference
7	78	152.4	[21]
10	64.4–93.2*	160.2 (after 80 cycles)	[22]
10	78	76**	[21]
20	62-72*	70**	
30	50-60*	87**	
40	50-60*	97**	
eutectic, 38.4 wt.%	58.3	136.8	[23]
eutectic, 41.3 wt.% (47 mol.%)	59.1	145	[24]
eutectic, 41.7 wt.%	59.0	132.2	[25]
eutectic, 49.3 wt.%	58.2	no data	[26]

* useful temperature range for PCM
** available specific enthalpy

Two different types of EG (matrix and flakes) to prepare composite EG/PCM (CPCM) samples were utilized in order to improve thermophysical properties of the selected mixture of 40 wt.% $MgCl_2 \cdot 6H_2O$ and 60 wt.% $Mg(NO_3)_2 \cdot 6H_2O$. In this case, expanded graphite meets nearly all requirements for a nucleating agent, therefore, its application for thermophysical properties improvement appears to be reasonable.

In order to provide the best way of preparing the composite EG/ inorganic PCM, different methods, usually applied for organic composite, including direct blending, vacuum impregnation, ultrasonic impregnation, and immersion, were studied in this research. The composite samples (CPCM) were proved to have excellent latent heat and significant reduction of the supercooling effect, which eliminates the need of nucleating agents. Moreover, the usage of EG suppresses significantly the melting time which indicates the heat transfer enhance of the mixture of 40 wt% of $MgCl_2 \cdot 6H_2O$ and 60 wt% of $Mg(NO_3)_2 \cdot 6H_2O$. All this allows empowering the utilization of the mentioned mixture in different fields of TES at low temperature.

2. Experimental

2.1. Materials

Both magnesium chloride $MgCl_2 \cdot 6H_2O$ and magnesium nitrate hexahydrate $Mg(NO_3)_2 \cdot 6H_2O$ were purchased from Merck (99.0 %). Expanded graphite (EG) flakes and matrix (Figure 1) were purchased from SGL Carbon, Germany.

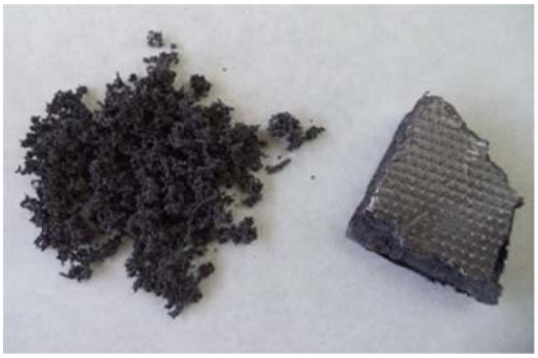

Figure 1. Expanded graphite flakes (left) and matrix (right).

2.2. Sample preparation

Both salts were dried at 40 °C for 12 hours with the subsequent placement in a desiccator. Then salts were grinded in a pounder and blended in the desired proportion (40/60 wt.%). After that, prepared mixtures were melted, well mixed and then crystallized again to ensure the composition homogeneity throughout the volume.

The CPCM samples were prepared using different techniques, including vacuum impregnation, ultrasound impregnation, immersion and direct blending. Two types of the expanded graphite were used: EG flakes in different weight fractions (5-10-15 wt.%) and EG matrix samples of 1x1x1 cm^3 each. Details of the samples preparation can be found in Table 2.

Table 2. Summary of CPCM samples preparation methods.

Graphite type				
Expanded graphite matrix			Expanded graphite flakes	
Preparation method				
Vacuum impregnation	Immersion	Ultrasound	Ultrasound	Direct blending
Experimental time, hours			**EG flakes, wt.%**	
0.25	1	0.25	5	5
0.5	3	0.5		
1	4	1	10	10
2	7	2		
4	12	3	15	15
7	24	7		

For vacuum impregnation, the solid salt mixture and the EG matrix samples were placed into the vacuum rotary evaporator (Rotavapor BUCHI R-210). The ultrasound impregnation was performed with an Ultrasonic Elmasonic S 30 (H). For this experiment, the mixture of inorganic salts and EG matrix samples were placed in a beaker inside the ultrasonic bath. For the immersion, EG matrix samples were put into a beaker with the molten salt mixture and were

contained in a THERMOSCIENTIFIC FD1500M oven. A number of samples was extracted depending on the experimental time. The obtained samples were abbreviated as $CPCM_{matrix}$.

As for EG flakes, different weight fractions (5-10-15 wt.%) of flake graphite was placed into a beaker containing the molten salt mixture with subsequent exposure to ultrasound or uniform and constant direct blending. The obtained samples were abbreviated as $CPCM_{flakes}$.

2.3. Morphological Characterization

A scanning electron microscope Jeol JSM6360 LV coupled to an energy dispersion spectrometer Inca Oxford was used to perform the chemical analysis of the samples. The experiments were carried out under the low vacuum with an electron beam of 20kV, 10 mm work distance, 60 mm spot size of 60 mm and backscattered electron signal.

2.4. Thermal properties

Measurements of melting temperature, heat of fusion, specific heat capacity, thermogravimetric analysis and analysis of cycling stability were conducted.

A DSC NETZSCH 204 Phoenix F1 with N_2 atmosphere (flow rate of 20 $mL \cdot min^{-1}$) was used to measure the phase change temperature and the latent heat of fusion/crystallization. The sample mass was of approximately 10 mg. The measurements were performed in a range from 20 °C to 130 °C. Sealed aluminum crucibles with capacity of 40 μL were utilized. Similarly, the DSC method was used to reveal the cycling stability of the samples between −15 °C and 130 °C, subjecting them to 3 heating-cooling cycles with the rate of 5 K/min.

Specific heat analysis was performed by means of DSC method, in the range from 20 °C to 130 °C. Sapphire was used as a reference material for the specific heat measurements. The samples of approximately 10 mg were placed to the sealed aluminum crucibles of 40 μL capacity. In order to measure the specific heat, there have been carried out three measurements for each sample: initially with an empty crucible to obtain a baseline, then with a reference material and the last one with an actual sample.

In addition to the DSC method, measurements with K-type thermocouples were performed to reveal the thermal performance of chosen mixtures with the larger amount of substance (about 7-8 g). The experimental scheme is presented in Figure 2.

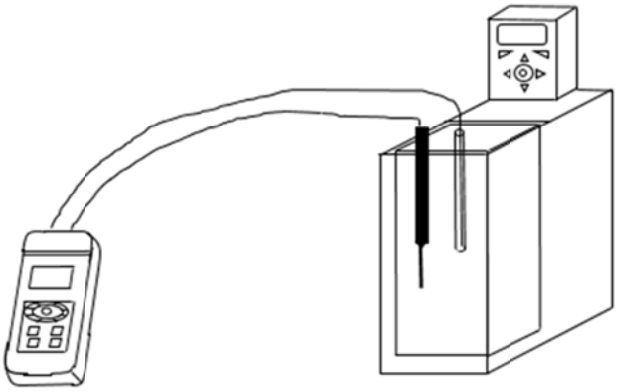

Figure 2. Scheme of experimental installation to characterize the thermal performance.

Thermal stability analysis was performed using a Mettler Toledo Model TGA/DSC1 1100 LF in the temperature range from 20 °C to 130 °C, under an atmosphere of purified nitrogen with flow rate of 30 mL/min. Aluminum crucibles with lids (40 μL) were used.

2.5. Determination of density and viscosity

The densities of solid salt mixtures were determined using a pycnometer with n-dodecane, while the liquid samples were evaluated by an oscillating densimeter (Mettler Toledo model ED50).

Brookfield Rheometer DV-III Ultra model was applied for measuring viscosity using a SC4-18 needle and Thermocel accessory was used to maintain the temperature. Analysis for different speeds of 10-80 rpm was performed.

3. Results and discussion

3.1. Morphological Characterization

The morphology of the samples studied is shown in Figure 3. EG flakes (Figure 3a) exhibit a wrinkled multiple layers surface texture, while the EG matrix (Figure 3b) has a more well-directed structure with a plurality of parallel layers. The structure of the CPCM samples is showed in Figure 3c and Figure 3d. The interlaminar space between graphite layers in EG provides channels for absorbing and retaining PCM. The inorganic PCM was intercalated into EG channel, interlayer and inner space easily, because of surface tension and capillary force at high temperature. The SEM and EDX analyzes revealed that all PCM was absorbed into channels and interlayers of EG. Due to excess of salt mixture, it is possible to see the individual salt particles, which remained outside, after the mixture completely filled the channels of EG. It should be emphasized that no differences were found between the different composite/EG preparation methods (vacuum impregnation, immersion, ultrasound, or mixing).

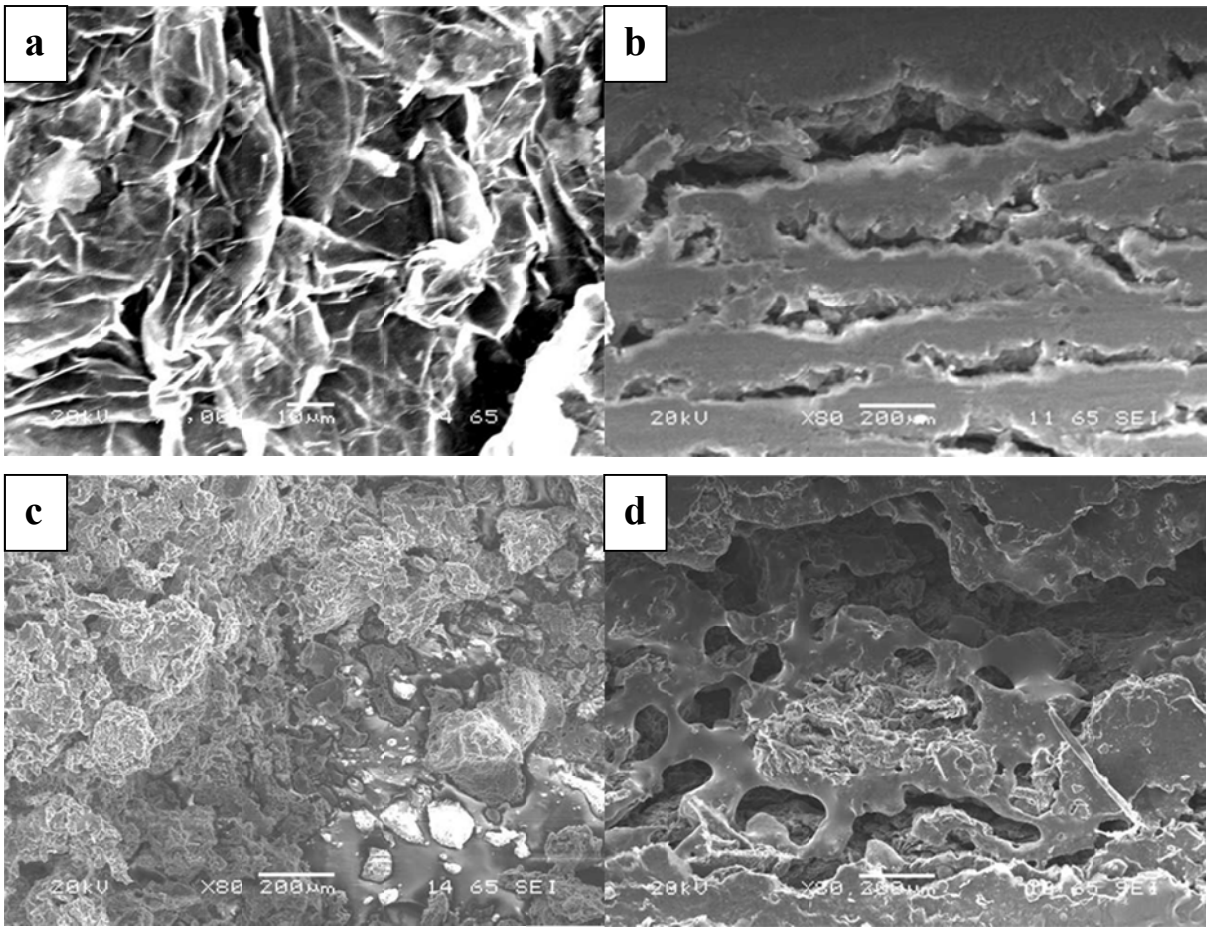

Figure 3. SEM images of (a) EG flakes, (b) EG matrix, (c) $CPCM_{flakes}$ of 5 wt.% of EG flakes and inorganic mixture, and (d) $CPCM_{matrix}$ (7 hours immersion).

The chemical composition of the prepared CPCM was further determined by EDX analysis attached to the SEM. The EDX spectrum sustains that the CPCM consists of C, O, Mg, Cl elements. Since spectra of the other samples present very similar result, Figure 4 shows an example of the EDX spectrum of the composite PCM/EG matrix ($CPCM_{matrix}$) sample (7 hours immersion). The strong O, Mg, and Cl signal originates from the inorganic mixture, while the C signal comes from the EG (Figure 4).

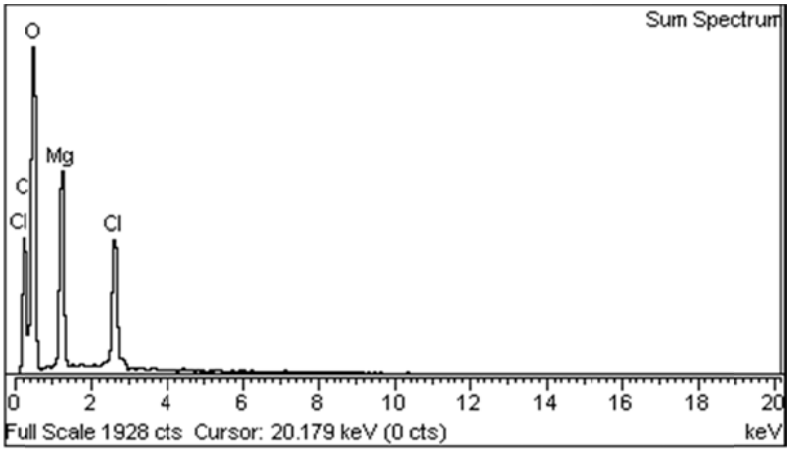

Figure 4. EDX spectra of the composite sample of EG matrix and inorganic mixture (7 hours immersion).

Figure 5 presents the XRD patterns of the EG in comparison to those of the pure PCM and the CPCM sample in the 2θ of 10.00 – 70.00°. The EG XRD patterns show a strong diffraction peak located at 26.596° (2θ) which is referred to the feature peak (002) of graphite [27]. The same diffraction peak can be observed in the pattern of the CPCM sample (Figure 5c). In the XRD pattern of the inorganic PCM strong diffraction peaks located at 20.042°, 27.029°, 30.527° (2θ), and 21.655°, 33.881° (2θ) are featured for $Mg(NO_3)_2 \cdot 6H_2O$ and $MgCl_2 \cdot 6H_2O$, respectively [28]. The XRD pattern of the composite sample includes the main diffraction peaks of magnesium nitrate hexahydrate, magnesium chloride hexahydrate and EG, but with the lower intensities than those in the original XRD patterns.

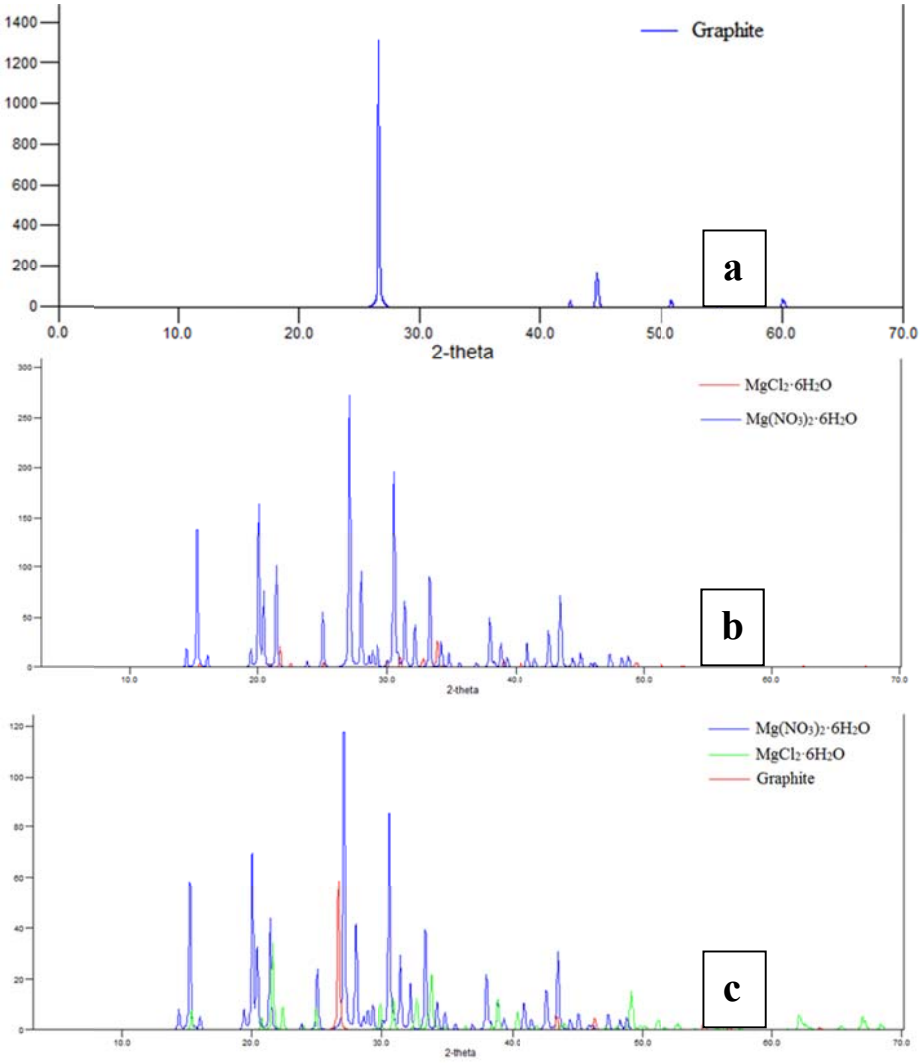

Figure 5. XRD patterns of (a) pure EG, (b) inorganic salt mixture 60 wt.% $MgCl_2 \cdot 6H_2O$ – 40 wt.% $Mg(NO_3)_2 \cdot 6H_2O$, and (c) composite CPCM sample.

3.2. Thermal properties

The specific heat capacity was determined to reveal the effect of EG addition on thermal properties. Specific heat capacities of pure PCM and CPCM samples varied with temperature are presented in Figure 6 and Figure 7. In solid state (298–320 K), the specific heat of the CPCM samples was close to the specific heat values of pure PCM, however the values for the $CPCM_{matrix}$ samples were slightly lower than those for the composite $CPCM_{flakes}$ samples (Table 3). On the other hand, in liquid state (345–400 K) the specific heat for all composite materials remains below the value of specific heat for pure PCM. In general, compared to pure binary mixture, the addition of EG obviously reduced the specific heat of samples.

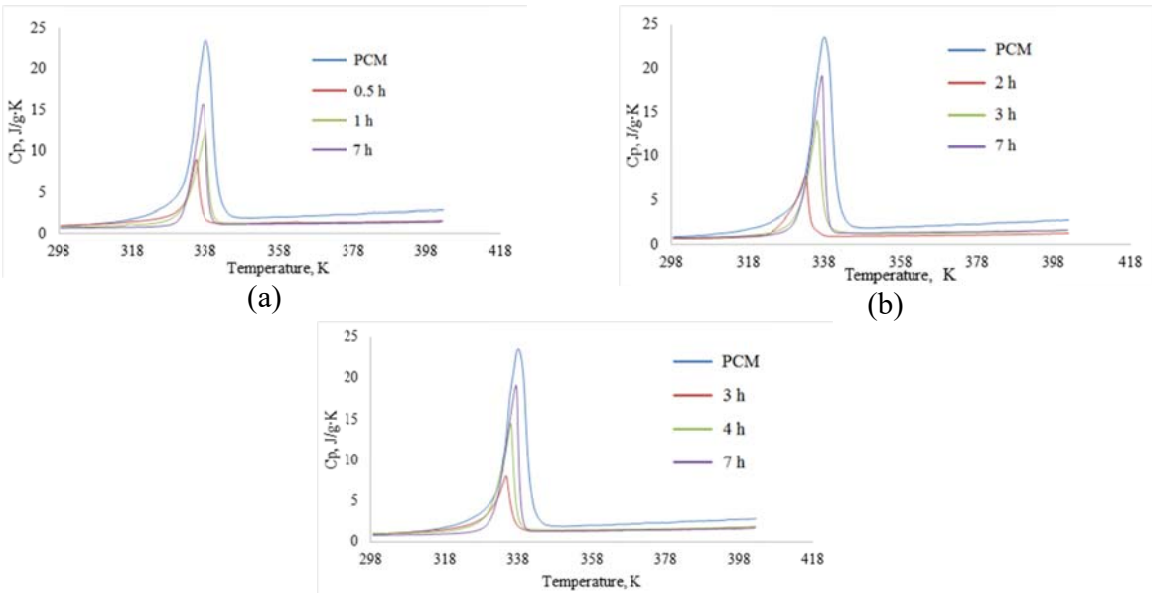

Figure 6. Specific heat capacity of the $CPCM_{matrix}$ samples prepared by (a) vacuum impregnation, (b) ultrasound, and (c) immersion, with different experimental times.

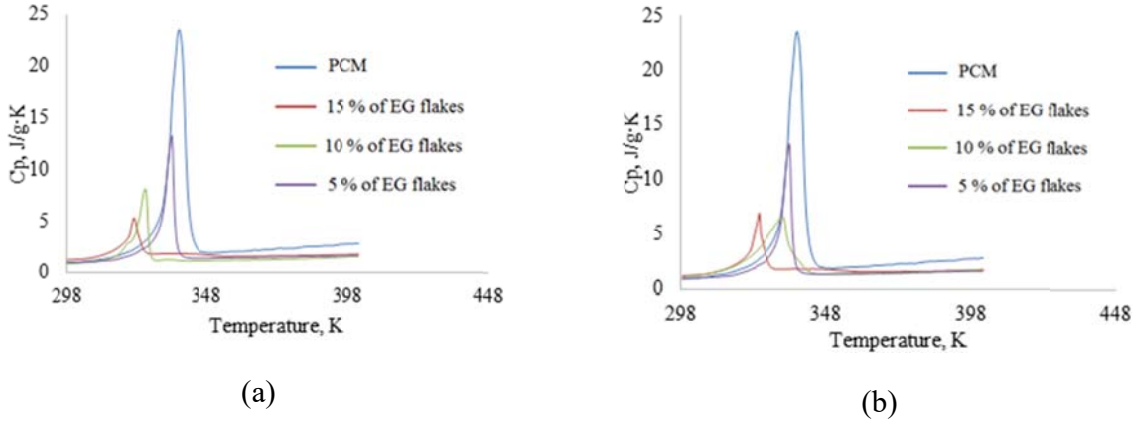

Figure 7. Specific heat capacity of the $CPCM_{flakes}$ samples prepared by (a) physical mixing, and (b) ultrasonic impregnation, with different EG content.

Table 3. Comparison of the specific heat capacity for pure PCM and CPCM samples in solid and liquid state.

Graphite type	**Preparation method**	**wt. % of EG**	**Cp at 298 K (solid state), [J·K^{-1}·g^{-1}]**	**Cp at 345 K (liquid state) [J·K^{-1}·g^{-1}]**
-	Pure PCM	-	0.91	2.16
EG matrix	vacuum *	-	0.68	1.14
	ultrasound *	-	0.75	1.25
	immersion *	-	0.83	1.36
EG flakes	physical mixing	5	1.01	1.38
		10	0.98	1.14
		15	1.23	1.78
	ultrasonic impregnation	5	0.98	1.38
		10	1.06	1.37
		15	1.23	1.82

*for 7 hours of exposure

In the phase change process, the specific heat decreased with the increase of EG content (Table 4). For the $CPCM_{matrix}$ samples, the specific heat values increase with the experimental time increasing, whereas for the composite samples with EG flakes, the specific heat increases with decreasing of EG percentage.

Table 4. Comparison of the specific heat capacity for pure PCM and CPCM samples in phase change process for $CPCM_{matrix}$ and for composites with flake EG.

Graphite type	**Preparation method**	**wt. % of EG**	**Phase change temperature [K]**	**Cp [J·K^{-1}·g^{-1}]**
-	Pure PCM	-	338	23.57
EG matrix	vacuum *	-	337	15.78
	ultrasound *	-	338	19.98
	immersion *	-	337	19.18
EG flakes	physical mixing	5	334	13.89
		10	326	8.08
		15	322	5.25
	ultrasonic impregnation	5	335	13.29
		10	333	6.66
		15	325	6.00

* for 7 hours of exposure

The most representative results of the composite samples thermal properties determination are included to Table 5. The table contains the average value for three heating/cooling cycles. The melting temperature of the composite samples with EG matrix is slightly different than that of pure PCM, but in general, the differences are not significant. Regarding the $CPCM_{flakes}$ samples, it was not possible to achieve reasonable and repeatable results using DSC method. It may be related to the fact that DSC method deals with a very small amount of material (about 10 mg), and considering that the volumetric amount of graphite flakes exceeds the volumetric amount of the PCM by several times, it may cause uncertainty in the results. To clarify this uncertainty the tests with K-type thermocouples were performed, which exhibited appropriate results and reveal that the EG flakes can still be used. Nevertheless, the problem of $CPCM_{flakes}$ sample preparation for DSC measurements should be addressed for getting the latent heat and phase change temperature data.

Considering the samples with EG matrix in their composition, it can be concluded that the optimal result of the encapsulation and enthalpy ratio can be reached with the experimental time of 1, 3 and 4 hours using the vacuum, ultrasound and immersion, respectively. In general, the percentage of encapsulation increases with the experimental time and with the EG percentage. Moreover, in the case of EG matrix, the heat of fusion/crystallization decreases with decreasing of experimental time, in other words, with the decreasing of the PCM content.

One of the important parameters of composite PCM is the impregnation efficiency, which can be defined by Eq. (1) [29]:

$$R = (\Delta H_{m,composite\ PCM} + \Delta H_{s,composite\ PCM})/(\Delta H_{m,pure\ PCM} + \Delta H_{s,pure\ PCM}) \qquad (1)$$

Therefore, the impregnation efficiency calculation results for the composite samples with EG matrix are reported in Table 5.

Table 5. Summary of melting/solidification temperatures, latent heat of fusion/solidification, supercooling (based on DSC study) and impregnation efficiency for $CPCM_{matrix}$ samples.

Sample	ΔH_m [kJ·kg^{-1}]	T_m [°C]	ΔH_s [kJ·kg^{-1}]	T_s [°C]	Supercooling [°C]	Impregnation efficiency [%]
pure PCM	132.5	62.0	120.8	27.9	34.1	-
Expanded graphite matrix						
Vacuum Impregnation						
0.5 h	106.7	63.5	106.8	46.5	17.0	84.3
1 h	114.7	64.3	115.2	46.1	18.2	90.7
7 h	114.6	63.2	112.1	46.1	17.2	89.5
Ultrasonic impregnation						
2 h	99.9	61.5	92.0	44.5	17.0	75.8
3 h	117.6	62.7	113.5	45.6	17.2	91.2
7 h	117.5	63.6	120.0	42.4	21.2	93.8
Immersion						
3 h	109.5	62.7	109.2	46.9	15.8	86.3
4 h	115.9	63.9	110.5	43.2	20.7	89.4
7 h	120.7	64.1	122.7	45.6	18.5	96.1
Expanded graphite flakes						
No satisfying data						

The melting and solidification DSC curves of the second cycle of the pure salt and the PCM/EG matrix are presented in Figure 8. In general, the DSC results of $CPCM_{matrix}$ samples present good reproducibility within cycling and minor deviations of the melting temperature and latent heat compared to the original mixture. In case of immersion, there is a tendency of increasing of CPCM latent heat as experimental time increases. In case of vacuum and ultrasonic impregnation this trend is not observed, which can be explained by the fact that these techniques provide much faster impregnation than the immersion method. Concerning the supercooling phenomena, the

results of DSC study show that the presence of EG reduces the difference between fusion and crystallization temperature up to 65%, acting as a nucleating agent.

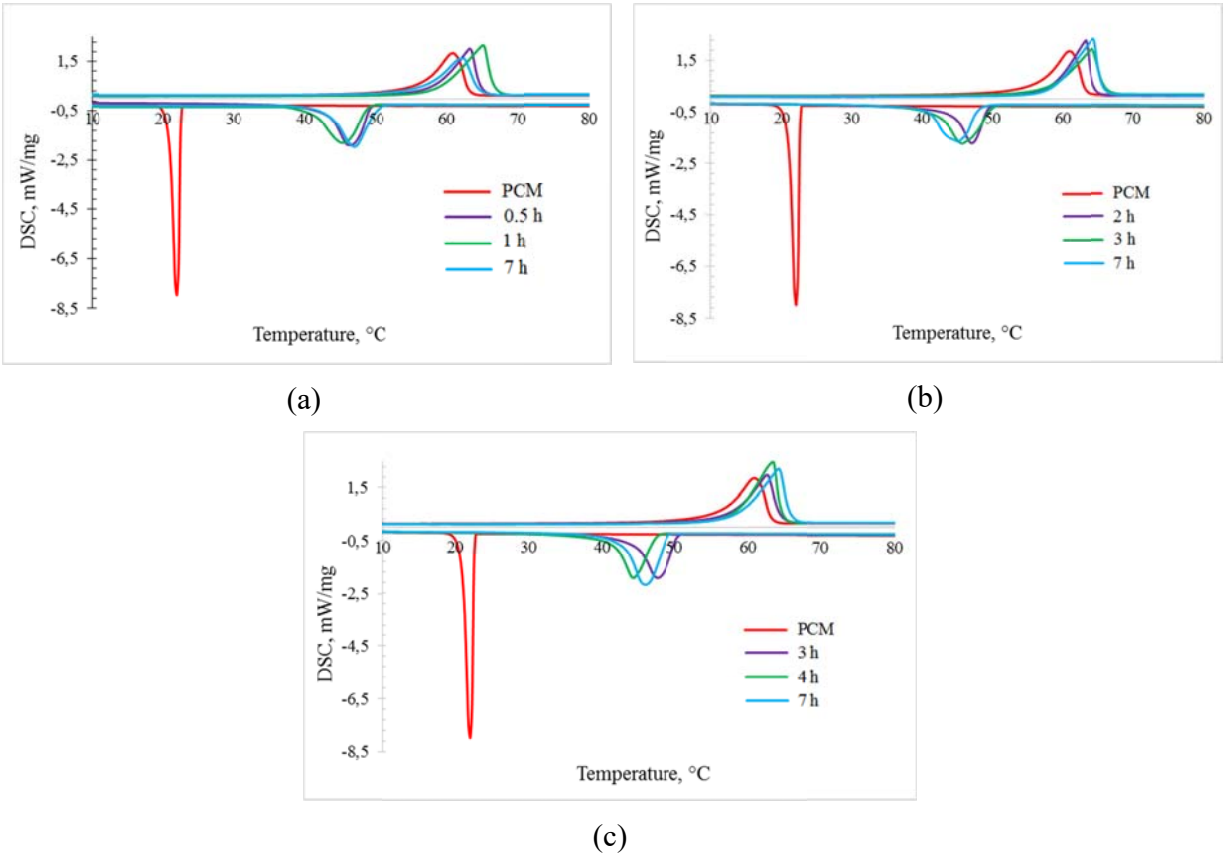

Figure 8. DSC curves of the composite PCM/EG matrix samples prepared by (a) vacuum impregnation, (b) ultrasound, and (c) immersion, with different experimental times

Two measurements of thermal stability were carried out with TGA for each sample, first in opened crucibles and then in sealed crucibles with a pierced lid. Eventually, all samples tested in sealed crucibles do not present any weight loss, i.e., they reach 130 °C with 100 % of the initial mass. Analysis in opened crucibles (Figure 9 and Figure 10) reveals that there is a slight weight loss which begins from about 80 °C and does not exceed 10 wt.% at 130 °C. That is why, for the practical applications of this mixture as PCM for TES it is recommended to use a closed system to avoid the mass loss.

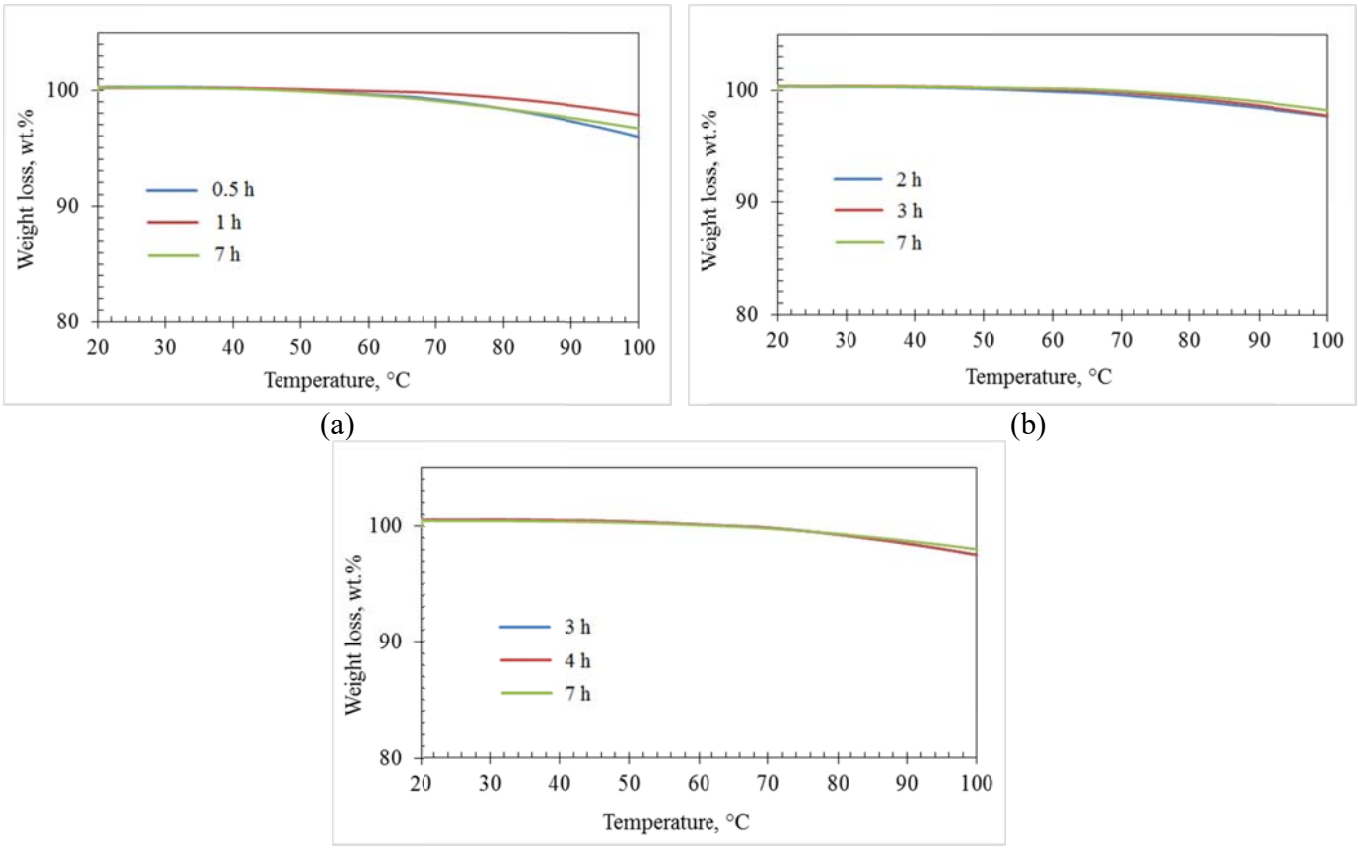

Figure 9. Thermal stability of the $CPCM_{matrix}$ samples prepared by (a) vacuum impregnation, (b) ultrasound, and (c) immersion, with different experimental times

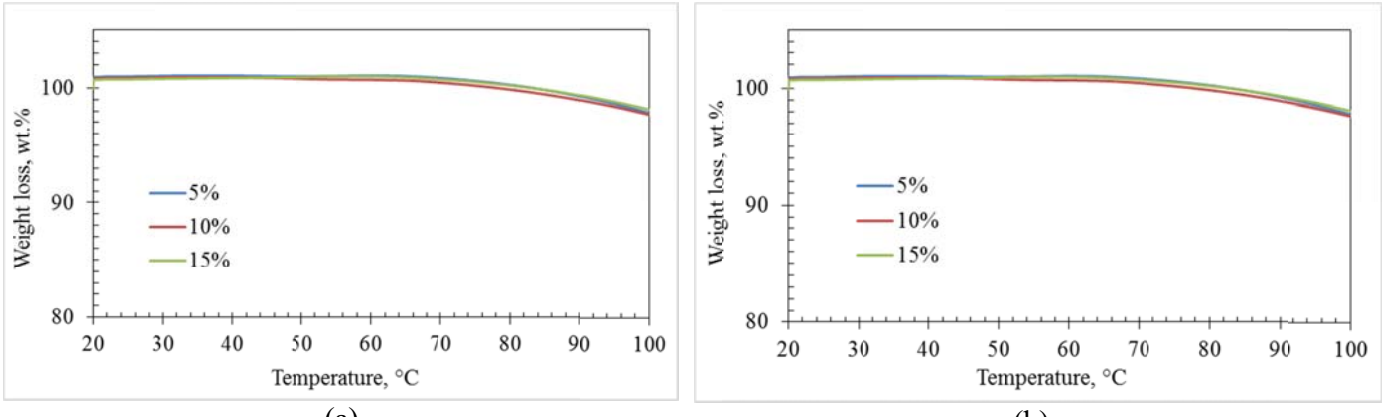

Figure 10. Thermal stability of the $CPCM_{flakes}$ samples prepared by (a) physical mixing, and (b) ultrasonic impregnation, with different EG content

In addition to the DSC method, tests with K-type thermocouples were carried out to reveal thermal performance of the composite PCM/EG samples. Temperature curves for pure PCM and $CPCM_{matrix}$ samples are shown in Figure 11. Comparing the curves of samples with vacuum exposure, it can be seen that the phase change process for pure PCM took about 700 s, while 579 s and 608 s for the composite samples of 0.5 and 7 hours of vacuum exposure respectively. In other words, the platform time of phase change was reduced by 17.3 % and 13.1 % for the composite samples of 0.5 and 7 hours of vacuum exposure, respectively (Figure 11a). With respect to the samples with ultrasound exposure, the phase change process for pure PCM took about 670 s, while 518 s and 585 s for the composite samples of 2 and 7 hours of ultrasound exposure, respectively. Thus, the platform time of phase change was reduced by 22.7 % and 12.7 % for the composite samples of 0.5 and 7 hours of ultrasound exposure, respectively. (Figure 11b). The phase change process for pure PCM took about 695 s, while 570 s and 605 s for the composite samples of 2 and 7 hours of immersion exposure, respectively. Thereby, the platform time of phase change was reduced by 18 % and 12.9 % for the composite samples of 0.5 and 7 hours of immersion exposure, respectively (Figure 11c). The cooling process shows that the pure PCM sample present significantly reduced supercooling of 4.0 °C compared with DSC studies (17 °C). The fact that the sample amount affects supercooling was already observed in previous works with inorganic salt hydrates and their mixtures: the larger the sample amount, more it reduces supercooling [30,31].

Additionally, the freezing curves (see Figure 11 a, b and c) reveal that in the $CPCM_{matrix}$ samples the supercooling effect disappears.

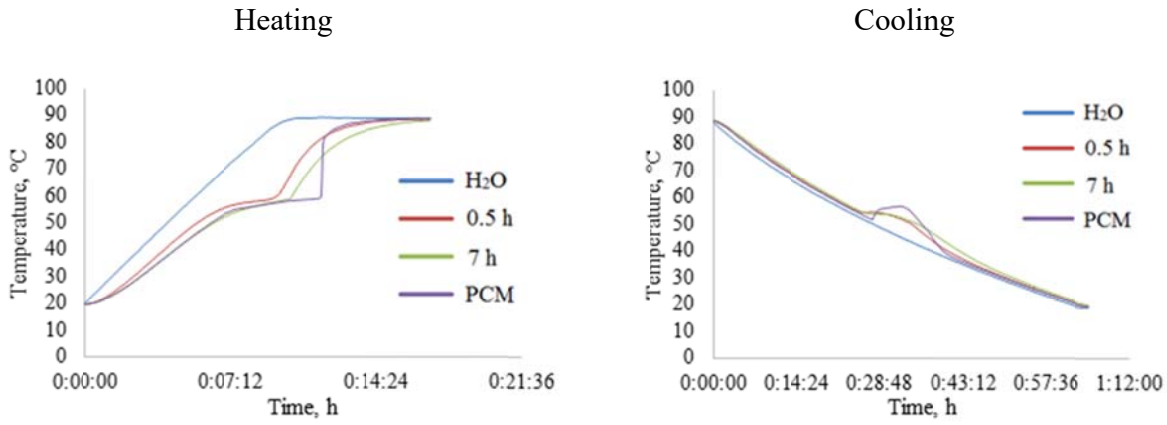

(a)

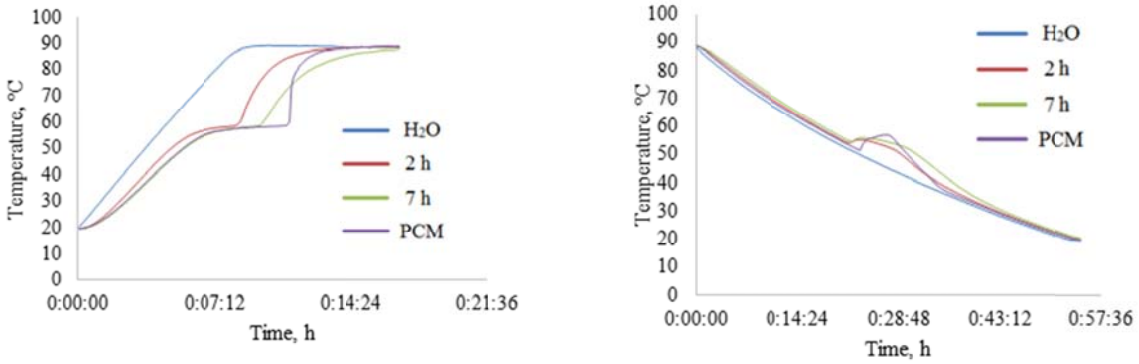

(b)

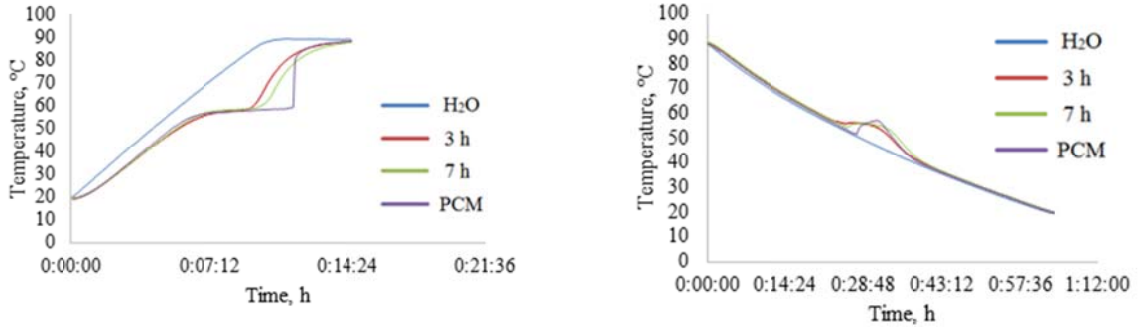

(c)

Figure 11. Comparison of heating and cooling curves of pure PCM and the composite PCM/EG matrix samples prepared by (a) vacuum impregnation, (b) ultrasound, and (c) immersion, with different experimental times. Water is used as reference material

The $CPCM_{flakes}$ samples show different thermal behavior than the composite samples with EG matrix. It can be seen that in addition to the significant decrease in the phase change platform, the heating rate of the sample with 15% of EG flakes approaches the heating rate of the reference material (water). The freezing curves in Figure 12 show the similar result. The longer freezing platform means the larger cooling time of CPCM.

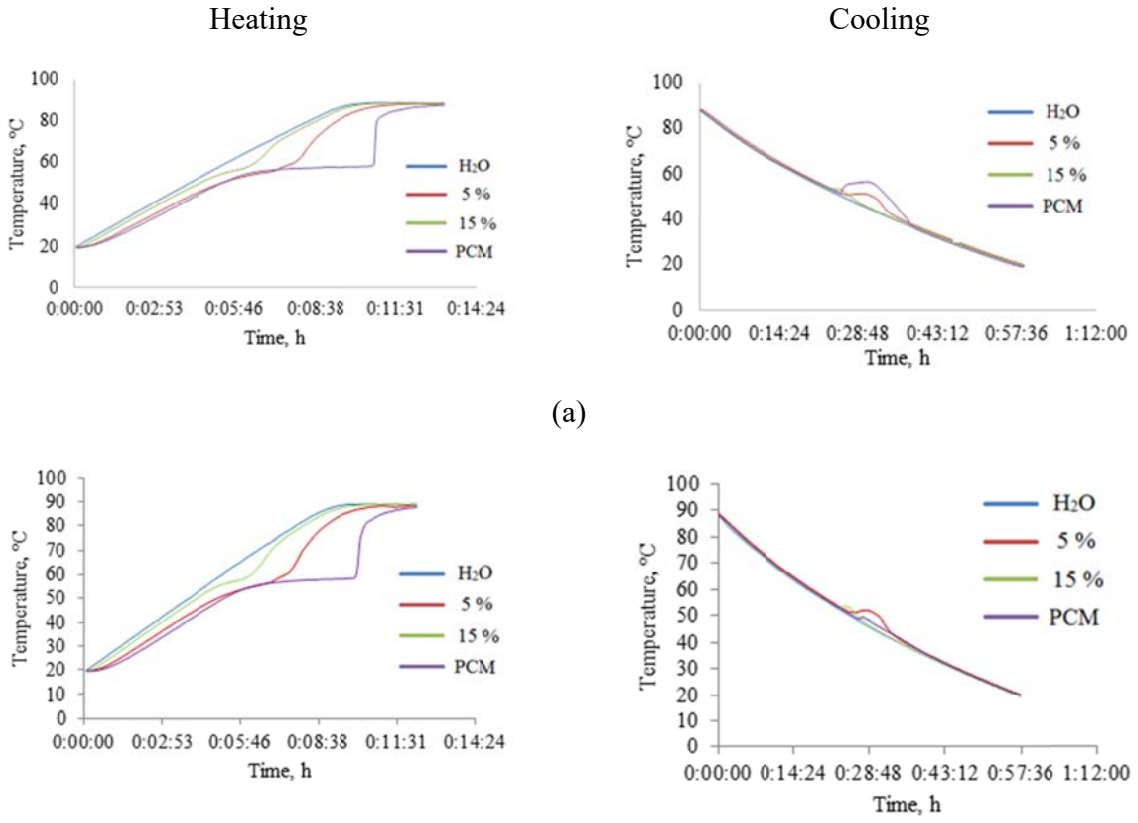

Figure 12. Comparison of heating and cooling curves of pure PCM and the $CPCM_{flakes}$ samples prepared by (a) physical mixing, and (b) ultrasonic impregnation, with different EG content.

3.3. Physical properties: density and viscosity

Solid samples densities were determined with a pycnometer and n-dodecane, while for the liquid samples, densities were measured by an oscillating densimeter Mettler Toledo ED50. Moreover, the temperature dependence of n-dodecane was measured with the same densimeter. Eq. (2) shows the n-dodecane density dependence on temperature:

$$\rho_n\ [kg \cdot m^{-3}] = 969.36 + 0.7045\ [T/K] \quad (2)$$

The results of density measurements are shown in Table 6.

Table 6. Summary of the densities of pure PCM (40 wt.% $MgCl_2 \cdot 6H_2O + Mg(NO_3)_2 \cdot 6H_2O$) and of EG samples.

T [ºC]	Density [kg·m^{-3}]		Phase
	40 wt.% $MgCl_2 \cdot 6H_2O + Mg(NO_3)_2 \cdot 6H_2O$	Expanded graphite	
ambient	1517	2.655	Solid
60	1518	-	Liquid
65	1515	-	
70	1512	-	

Viscosity measurements were performed with pure PCM (40 wt.% $MgCl_2 \cdot 6H_2O$ + $Mg(NO_3)_2 \cdot 6H_2O$) in the range from 60 °C to 110 ºC (Table 7). The results of measurements of density and viscosity are summarized in Figure 13.

Table 7. Viscosity values at different temperatures for the mixture of 40 wt.% $MgCl_2 \cdot 6H_2O + Mg(NO_3)_2 \cdot 6H_2O$.

Viscosity [cP]	Velocity [RPM]	Shear strength [D/cm^2]	Temperature [°C]
38.31	50.00	24.72	60
31.70		20.46	65
27.57		17.79	70
22.38		14.44	80
19.23		12.41	90
21.02		13.56	100
20.83		13.44	110

According to the expectations, viscosity decreases with increasing the temperature and moreover, viscosity values do not depend on torque speed which indicates the Newtonian behavior of the studied PCM. That is why, Table 7 and Figure 13 only show the results for the speed of 50 rpm. Viscosity values of the molten salt mixture decrease from 38.2 to 20.7 mPa·s in the temperature range from 60 °C to 110 °C.

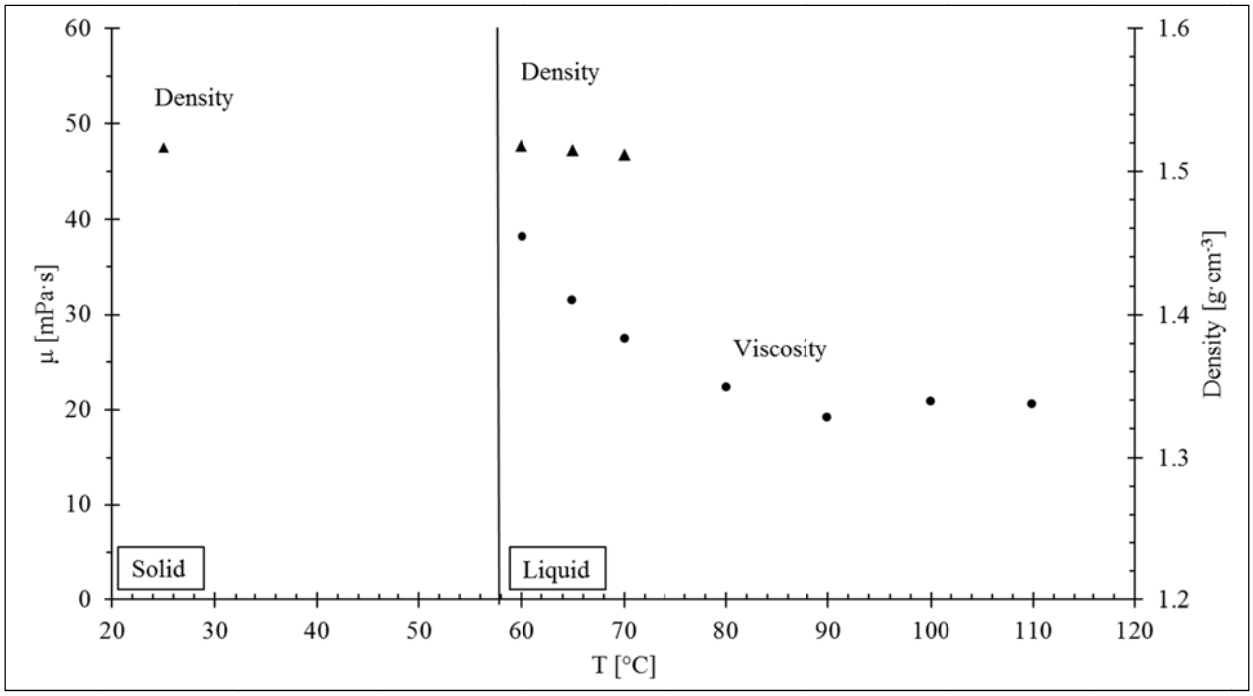

Figure 13. Temperature dependence of the dynamic viscosity and density of pure PCM (40 wt.% $MgCl_2 \cdot 6H_2O$+$Mg(NO_3)_2 \cdot 6H_2O$).

4. Conclusions

In this study, an inorganic mixture of 40 wt.% $MgCl_2 \cdot 6H_2O$ and 60 wt.% $Mg(NO_3)_2 \cdot 6H_2O$ was impregnated into two types of the expanded graphite: flakes of the EG and the EG matrix. The composite CPCM samples, prepared by five different techniques, including vacuum impregnation, ultrasound impregnation, immersion, and physical mixing, were compared.

Considering the samples with EG matrix, it can be concluded that the optimal result of the encapsulation and ΔH ratio can be reached with the experimental time of 1 h, 3 h and 4 h using the vacuum, ultrasound and immersion methods, respectively. Moreover, the percentage of encapsulation increases with the experimental time and with the EG percentage for the EG matrix and for the EG flakes, respectively. Concerning the supercooling phenomena, the results show that the presence of EG reduces the difference between fusion and crystallization temperature for up to 65%, acting as a nucleating agent. As for $CPCM_{flakes}$ samples, it was not possible to achieve reasonable and repeatable results using DSC method. It may be related to the fact that DSC method deals with a very small amount of material (about 10 mg), and considering that the volumetric amount of graphite flakes exceeds the volumetric amount of the PCM by several times, it may cause uncertainty in the results. To clarify this uncertainty the tests with K-type thermocouples were performed, which exhibited appropriate results and reveal that the EG flakes can still be used to improve thermophysical properties. Nevertheless, the problem of $CPCM_{flakes}$ sample preparation for DSC measurements should be addressed for getting the latent heat and phase change temperature data.

TG analysis for both types CPCM samples in opened crucibles reveals that there is a slight weight loss which begins from about 80 °C and does not exceed 10 wt.% at 130 °C, while in closed crucibles the sample mass remains the same. That is why, for the practical applications of this mixture as PCM for TES it is recommended to use a closed system to avoid the mass loss.

The results with K-type thermocouple measurements show that for the pure PCM there is a significate decrease in supercooling (4 °C) compared to the results of the DSC (34.1 °C). The measurements for the $CPCM_{matrix}$ and $CPCM_{flakes}$ show that the subcooling disappears completely, which eliminates the use of nucleating agents. Moreover, using EG suppresses significantly the melting time which indicates the heat transfer enhance of the mixture.

Acknowledgements

Authors from Universidad de Antofagasta thank CONICYT/FONDAP N° 15110019, ERANET-LAC 2015-2016, project ELAC2015/T06-0988 and CONICYT/FONDECYT/REGULAR N° 1170675 for the financial support. Yana Galazutdinova would like to acknowledge for her doctorate scholarship to the CONICYT-PCHA/Doctorado Nacional para Estudiantes Extranjeros 2014/Folio 63140052. The work was partially funded by the Spanish government (ENE2015-64117-C5-1-R (MINECO/FEDER)). Dr. Luisa F. Cabeza would like to thank the Catalan Government for the quality accreditation given to her research group (2014 SGR 123). GREA is certified agent TECNIO in the category of technology developers from the Government of Catalonia. This project has received funding from the European Commission Seventh Framework Programme (FP/2007-2013) under Grant agreement NºPIRSES-GA-2013-610692 (INNOSTORAGE) and from the European Union's Horizon 2020 research and innovation programme under grant agreement No 657466 (INPATH-TES).

References

[1] Lane, G.A. (1991). Phase Change Material for Energy Storage Nucleation to Prevent Supercooling. *Solar Energy Materials and Solar Cells, 27*, 135-160.

[2] Pilar, R., Svoboda, L., Honkova, P., Oravova, L. (2012). Study of magnesium chloride hexahydrate as heat storage material. *Thermochimica acta, 546,* 81-86.

[3] Fan, L., Khodadadi, J.M. (2011). Thermal conductivity enhancement of phase change materials for thermal energy storage: A review. *Renewable and Sustainable Energy Reviews, 15* (1), 24-46.

[4] Al-Shannaq, R., Kurdi, J., Al-Muhtaseb, S., Dickinson, M., Farid, M. (2015). Supercooling elimination of phase change materials (PCMs) microcapsules. *Energy, 87* (1), 654-662.

[5] Cabeza, L.F., Mehling, H., Hiebler, S., Ziegler, F. (2002). Heat transfer enhancement in water when used as PCM in thermal energy storage. *Applied thermal engineering, 22* (10), 1141-1151.

[6] Tian, H., Wang, W., Ding, J., Wei, X., Huang, C. (2016). Preparation of binary eutectic chloride/expanded graphite as high-temperature thermal storage materials. *Solar Energy Materials and Solar Cells, 149,* 187-194.

[7] Li, Z., Wu, Z.G. (2016). Development of medium-temperature composite phase change material with high thermal stability and conductivity. *Solar Energy Materials and Solar Cells, 155*, 341–347.

[8] Tian, H,, Wang, W., Ding, J., Wei, X., Song, M., Yang, J. Thermal conductivities and characteristics of ternary eutectic chloride/expanded graphite thermal energy storage composites (2015). *Applied Energy, 148,* 87–92.

[9] Kim, D., Jung, J., Kim, Y., Lee, M., Seo, J., Khan, S.B. (2016). Structure and thermal properties of octadecane/expanded graphite composites as shape-stabilized phase change materials. *International Journal of Heat and Mass Transfer, 95,* 735–741.

[10] Ramakrishnan, S., Sanjayan, J., Wang, X., Alam, M., Wilson, J. (2015). A novel paraffin/expanded perlite composite phase change material for prevention of PCM leakage in cementitious composites. *Applied Energy, 157,* 85–94.

[11] Wu, S., Li, T.X., Yan, T., Dai, Y.J., Wang, R.Z. (2016). High performance form-stable expanded graphite/stearic acid composite phase change material for modular thermal energy storage. *International Journal of Heat and Mass Transfer, 102,* 733–744.

[12] Chen, C., Zhang, H., Gao, X., Xu, T., Fang, Y., Zhang, Z. (2016). Numerical and experimental investigation on latent thermal energy storage system with spiral coil tube and paraffin/expanded graphite composite PCM. *Energy Conversion and Management, 126,* 889–897.

[13] Gao, L., Zhao, J., An, Q., Zhao, D., Meng, F., Liu, X. (2017). Experiments on thermal performance of erythritol/expanded graphite in a direct contact thermal energy storage container. *Applied Thermal Engineering, 113,* 858–866.

[14] He, Y., Zhang, X., Zhang, Y., Song, Q., Liao, X. (2016). Utilization of lauric acid-myristic acid/expanded graphite phase change materials to improve thermal properties of cement mortar. *Energy and Buildings, 133,* 547–558.

[15] Liu, C., Yuan, Y., Zhang, N., Cao, X., Yang, X. (2014). A novel PCM of lauric–myristic–stearic acid/expanded graphite composite for thermal energy storage. *Materials Letters, 120,* 43–46.

[16] Zhang, H., Gao, X., Chen, C., Xu, T., Fang, Y., Zhang, Z. (2016). A capric–palmitic–stearic acid ternary eutectic mixture/expanded graphite composite phase change material for thermal energy storage. *Composites Part A: Applied Science and Manufacturing, 87,* 138–145.

[17] Sobolciak, P., Mrlík, M., Al Maadeed, M.A., Krupa, I. (2015). Calorimetric and dynamic mechanical behavior of phase change materials based on paraffin wax supported by expanded graphite. *Thermochimica Acta, 617,* 111–119.

[18] Sari, A., Karaipekli, A. (2009). Preparation, thermal properties and thermal reliability of palmitic acid/expanded graphite composite as form stable PCM for thermal energy storage. *Solar Energy Materials and Solar Cells, 93* (5), 571–576.

[19] Zhuo, L., Zhi-Gen, W. (2016). Development of medium-temperature composite phase change material with high thermal stability and conductivity. *Solar Energy Materials and Solar Cells, 155*, 341-347.

[20] Heqing, T., Weilong, W., Jing D., Xiaolan, W., Chenglong, H. (2016). Preparation of binary eutectic chloride/expanded graphite as high-temperature thermal energy storage materials. *Solar Energy Materials and Solar Cells, 149*, 187–194.

[21] Nagano, K., Ogawa, K., Mochida, T., Hayashi, K., Ogoshi, H. (2004). Thermal characteristics of magnesium nitrate hexahydrate and magnesium chloride hexahydrate mixture as a phase change material for effective utilization of urban waste heat. *Applied Thermal Engineering, 24,* 221–232.

[22] Nagano, K., Ogawa, K., Mochida, T., Hayashi, K., Ogoshi, H. (2004). Performance of heat charge/discharge of magnesium nitrate hexahydrate and magnesium chloride hexahydrate mixture to a single vertical tube for a latent heat storage system. *Applied Thermal Engineering, 24,* 209–220.

[23] Zhou, Q., Yin, X., Wang, Q., Wang, C. (2011). Phase Diagram Prediction of the System Mg(NO3)2-MgCl2-H2O as Phase Change Materials. *Acta Chimica Sinica, 69* (15), 1725-1730.

[24] Yoneda, N., Takanashi, S. (1978). Eutectic mixtures for solar heat storage. *Solar Energy, 21* (1), 61-63.

[25] Jotshi, C. K., Goswami, D. Y., Tomlinson, J. J. (1992). In Proc. American Solar Energy Society Annual Conf., USA.

[26] Lane, G. A. (1983). Solar Heat Storage: Latent Heat Materials, CRC Press Inc., USA.

[27] Howe, J.Y., Rawn, C.J., Jones, L.E., Ow, H. (2003). Improved crystallographic data for graphite. *Powder Diffraction, 18* (2), 150-154.

[28] http://webmineral.com/ last visit may 2017.

[29] Zhong, L., Zhang, X., Luan, Y., Wang, G., Feng, Y., Feng, D. (2014). Preparation and thermal properties of porous heterogeneous composite phase change materials based on molten salts expanded graphite. *Solar Energy, 14* (107), 63–73.

[30] Rathgeber, C., Schmit, H., Miro, L., Cabeza, L.F., Gutierrez, A., Ushak, S., Hiebler, S., Hauer, A. Analysis of supercooling of phase change materials with increased sample size – Comparison of

measurements via DSC, T-History and at pilot plant scale. Greenstock 2015 - 13th IEA ECES Conference, At Beijing, China.

[31] Galazutdinova, Y., Grágeda, M., Cabeza, L.F., Ushak, S. (2017). Novel inorganic binary mixture for low temperature heat storage applications. *International Journal of Energy Research*, in press.